ID4100 Project Report
Fractal Acoustic Meta-materials for noise suppression and absorption

Abhyudit Singh Manhas - ME18B088
Guide: Dr. P Chandramouli

1 Introduction

A metamaterial is any material that is engineered to have a property not usually found in naturally occurring materials. They are made from assemblies of multiple elements, which are themselves made from composite materials such as metals and plastics. The materials are usually arranged in repeating patterns, at scales that are smaller than the wavelengths of the phenomena they influence. Metamaterials derive their properties not from their base materials, but from their newly designed structures. Their precise shape, geometry, size, orientation and arrangement gives them their smart properties capable of manipulating electromagnetic/sound waves: by blocking, absorbing, enhancing, or bending waves. They can achieve benefits that go beyond what is possible with conventional materials. Appropriately designed metamaterials can affect waves of electromagnetic radiation or sound in a manner not observed in bulk materials. Potential applications of metamaterials are diverse and include optical filters, medical devices, remote aerospace applications, sensor detection and infrastructure monitoring, smart solar power management, crowd control, high-frequency battlefield communication and lenses for high-gain antennas, improving ultrasonic sensors, and even shielding structures from earthquakes.
In a similar vein, acoustic metamaterials are defined to be a class of artificially periodic structures that exhibit extraordinary elastic and physical properties which cannot be easily found in naturally occurring materials. Because of their special physical properties, they have very high development prospects in many potential fields such as sound insulation and absorption, vibration and noise reduction. Hierarchical or fractal construction with multiple length scales is widespread and has been used in optical and mechanical fields because of its excellent sub-wavelength and multi-band characteristics. Therefore, the self-similar fractal technique is applied to design the acoustic metamaterial. In this project, porous fractal acoustic metamaterials, and their possible use in sound attenuation and absoprtion is investigated. The fractal curve of interest is a Sierpiński carpet. This is very similar in construction to a Micro-perforated panel (MPP) absorber. A MPP is basically a thin flat plate, perforated with a lattice of short narrow tubes (usually circular), whose specific acoustic impedance can be derived from the particle velocity through the tubes. The perforations of a MPP provide enough acoustic resistance and low acoustic mass reactance, which are necessary for wide-band sound absorption.
Hence, a porous fractal acoustic metamaterial, with the fractal curve being a Sierpiński carpet, is proposed for broadband sound attenuation. In the next section, some information about fractal curves in general, and the Sierpiński carpet in particular, is presented.

2 Fractal Curves - Sierpinski Carpet

A fractal curve is a mathematical curve whose shape retains the same general pattern of irregularity, regardless of how high it is magnified, that is, its graph takes the form of a fractal. Fractals appear the same at different scales, as illustrated in successive magnifications of the Mandelbrot set. Fractals often exhibit similar patterns at increasingly smaller scales, a property called self-similarity, also known as expanding symmetry or unfolding symmetry; if this replication is exactly the same at every scale. In general, fractal curves do not have a finite length. Fractal curves and fractal patterns are widespread in nature, and are found in places such as broccoli,

snowflakes, feet of geckos, frost crystals, and lightning bolts.
The fractal curve used in our porous acoustic metamaterial is a Sierpiński carpet. The Sierpiński carpet after the 5th iteration is shown below.

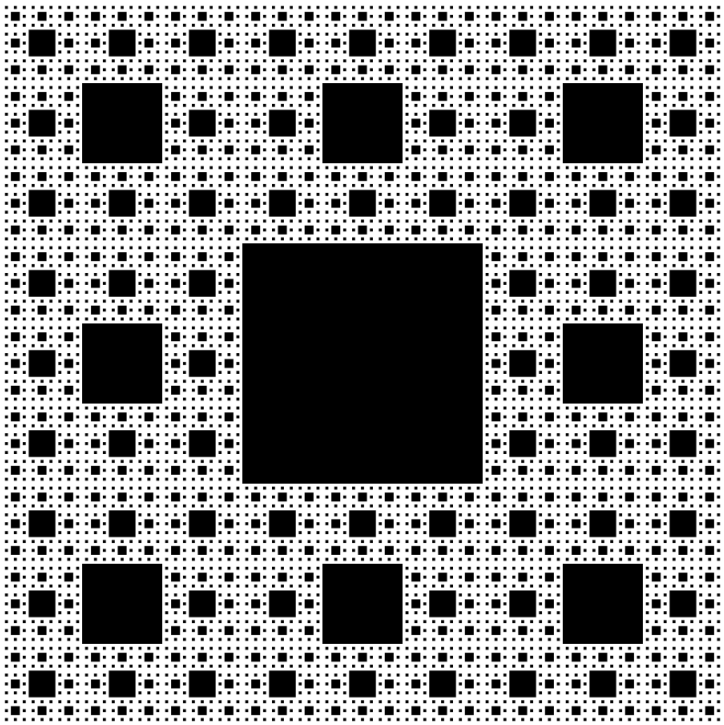

Figure 1: Sierpiński carpet after 5th iteration/order 5

The basic technique behind generating the Sierpiński carpet involves subdividing a square into smaller copies of itself, removing one or more copies, and then continuing recursively. The exact procedure is as follows:
1) Begin with a square of size $a \times a$
2) Cut the square into 9 congruent subsquares in a 3-by-3 grid
3) Remove the central subsquare
4) Apply the same procedure recursively to the remaining 8 subsquares.
A MATLAB program was developed that generates the Sierpiński carpet of order N. The program assumes an origin to be at the bottom left corner of the square. Then for the nth iteration, where $n = 1, 2, \ldots, N$, it finds the (x, y) coordinates of the centre of each square hole. The square holes will have length $L\left(= \dfrac{a}{3^n}\right)$, and the centre coordinates lie uniformly between $\dfrac{3L}{2}$ and $a - \dfrac{3L}{2}$. However, there will be some centres that will lie in regions from which square holes have already been removed in the previous iteration. So, these centres are deleted if they are in the vicinity of the centres from the previous iteration. Also the coordinates of the vertices with respect to the centres are simply $\left(\pm\dfrac{L}{2}, \pm\dfrac{L}{2}\right)$. Note that L can only take values from $\dfrac{a}{3}, \dfrac{a}{3^2}, \ldots, \dfrac{a}{3^N}$. Therefore, the coordinates of the vertices of the square holes with respect to the origin at the bottom left are simply given by

$$(x_v, y_v) = (x, y) + \left(\pm\frac{L}{2}, \pm\frac{L}{2}\right)$$

where (x, y) are the centre coordinates of the particular square hole. The holes are then created using the 'fill' command in MATLAB. Also, the centres and edge lengths of each square hole are stored in a variable named 'data'. These values stored are then subsequently used to 3D print the specimen. The Sierpiński carpet of order $1, 2 \ldots, 6$ generated from the program are now shown below.

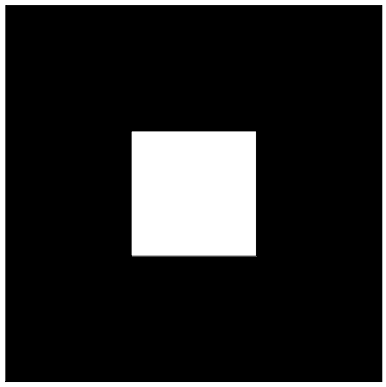

Figure 2: Sierpiński carpet of order $N = 1$

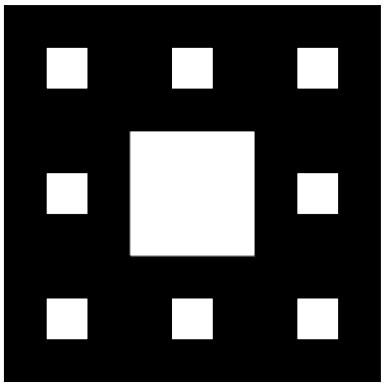

Figure 3: Sierpiński carpet of order $N = 2$

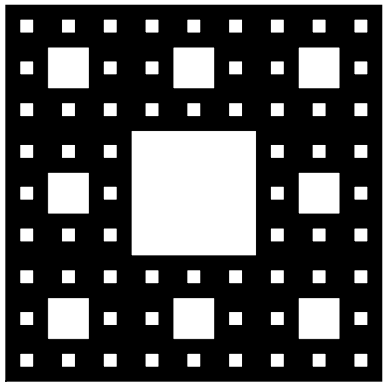

Figure 4: Sierpiński carpet of order $N = 3$

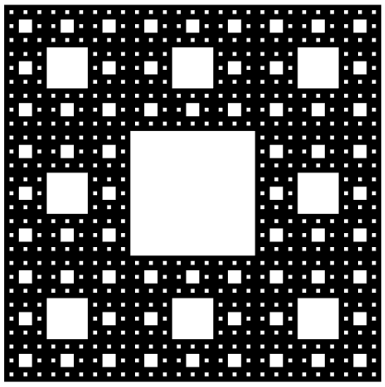

Figure 5: Sierpiński carpet of order $N = 4$

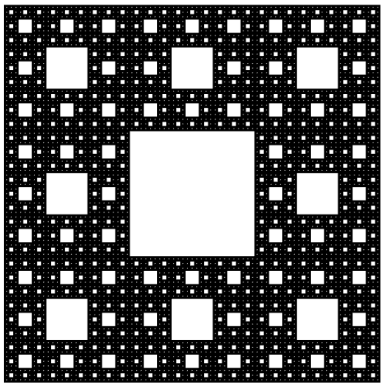

Figure 6: Sierpiński carpet of order $N = 5$

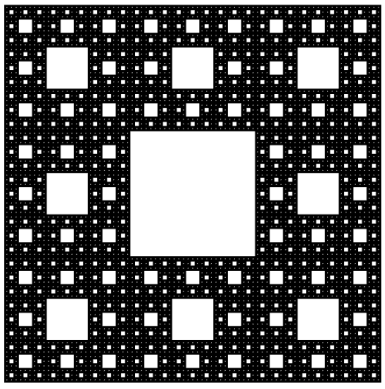

Figure 7: Sierpiński carpet of order $N = 6$

The area of the Sierpiński carpet of order N is

$$A_n = \left(\frac{8}{9}\right)^n A_0 = \left(\frac{8}{9}\right)^n a^2 \tag{1}$$

Thus, as $N \to \infty$, the area of the carpet goes to 0.

3 Eigen-frequency Analysis

Now, an eigen-frequency analysis of a cuboidal air cavity, which has this pattern on one of its square faces, is conducted in the finite-element software ABAQUS. For a cuboidal cavity of dimensions L_x, L_y and L_z with one face along the z-axis completely open (pressure release boundary condition), the eigen-frequencies are given by

$$f_{lmn} = \frac{c}{2\pi}\sqrt{\left(\frac{l\pi}{L_x}\right)^2 + \left(\frac{m\pi}{L_y}\right)^2 + \left(\frac{(2n+1)\pi}{2L_z}\right)^2}, \qquad l, m, n = 0, 1, 2, \ldots \tag{2}$$

where c is the speed of sound. For our particular cavity,

$$L_x = L_y = 100 \text{ mm}$$

and the length of the cavity along the z-axis (L_z) and the order of the Sierpiński carpet N is varied. Since ABAQUS scripting is done using Python, all programs are written in Python to generate the part geometry and set up the simulations. The part in ABAQUS is made by drawing the square face, and then extruding it by L_z. The holes are then sketched on one of the square faces, using the information about the centre coordinates and the edge lengths of each square hole as discussed in the previous section. Then in the Property module, the material behaviour 'acoustic medium' is chosen, with

$$\rho = 1.225 \text{ kg/m}^3, \; B = 142 \text{ kPa}$$

which are the standard values for Air. Following this, the part is meshed. The mesh should be adequately refined for reasonable accuracy. An 'internodal interval' is defined as the distance from a node to its nearest neighbor in an element. It is the element size for a linear element and half of the element size for a quadratic element. At a fixed internodal interval, quadratic elements are more accurate than linear elements. Thus we use 10-noded quadratic tetrahedral elements for meshing, with the mesh being finer in and around the square holes. We have the following relation

$$L_{max} < \frac{c}{10 f_{max}}$$
$$\implies \Omega_{max} < \frac{c}{5 f_{max}}$$

where L_{max} is the maximum internodal interval of an element in the mesh, Ω_{max} is the maximum size of the quadratic element, c is the speed of sound, and f_{max} is the maximum frequency of interest. We wish to search all the eigen-frequencies till 5000 Hz, i.e.

$$f_{max} = 5000 \text{ Hz}$$
$$\implies \Omega_{max} < 0.0136$$

Hence, the maximum element size should not exceed 13.6 mm. Since the surfaces for an acoustic medium in ABAQUS are rigid by default, no velocity boundary conditions need to be specified. However, a pressure release boundary condition ($p = 0$) is applied to each of these square holes. The values of L_z for this analysis are 50, 100, 200 and 300 mm, with N being 2, 3 and 4. The final part and its mesh for $L_z = 200$ mm and $N = 3$ are shown below.

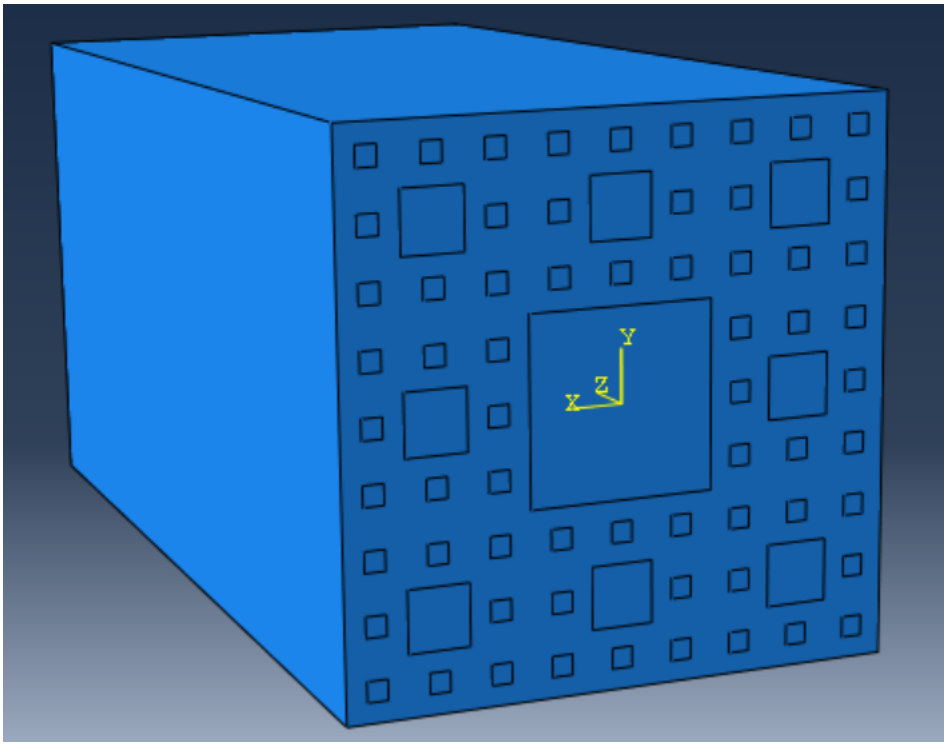

Figure 8: The cuboidal cavity in ABAQUS viewport

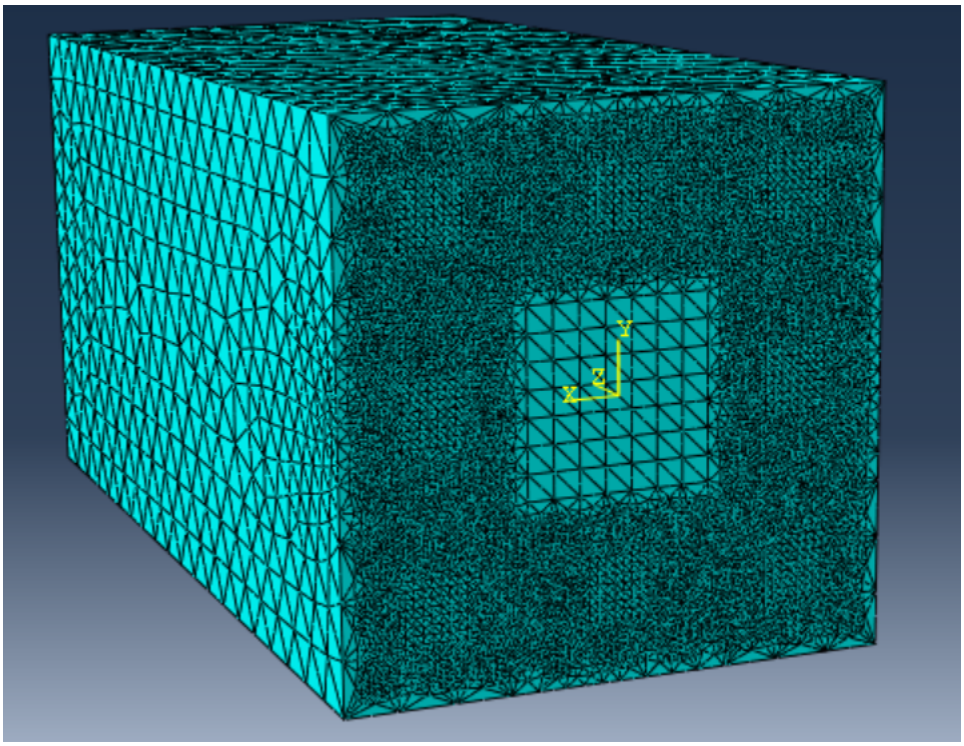

Figure 9: Mesh of the cuboidal cavity

The eigen-frequencies for the part are now computed in the range from 0 to 5000 Hz. This is done by selecting the 'Procedure type' as 'Linear perturbation' and choosing the 'Frequency' step, in the Step module. The results are also compared with the case when that entire face is fully open (Eq.(2)).

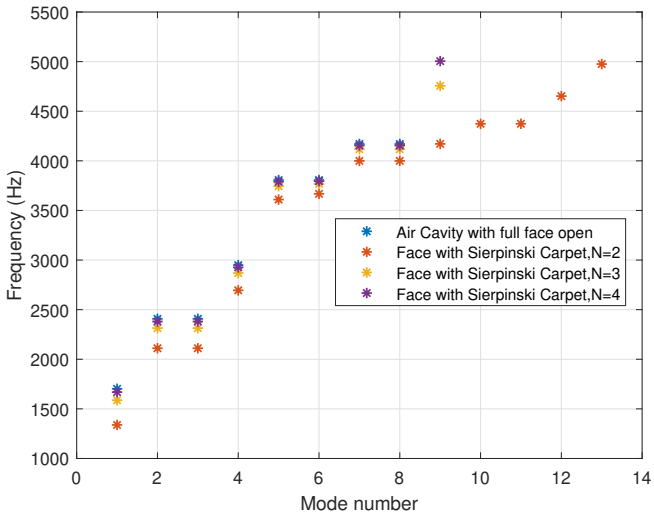

Figure 10: Eigen-frequencies for $L_z = 50$ mm

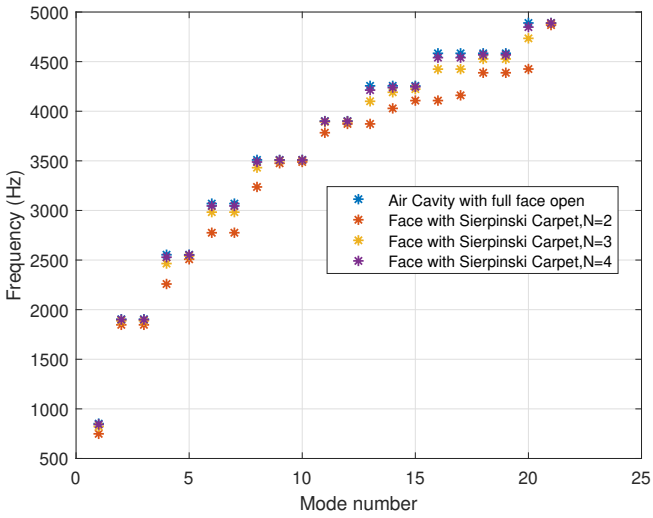

Figure 11: Eigen-frequencies for $L_z = 100$ mm

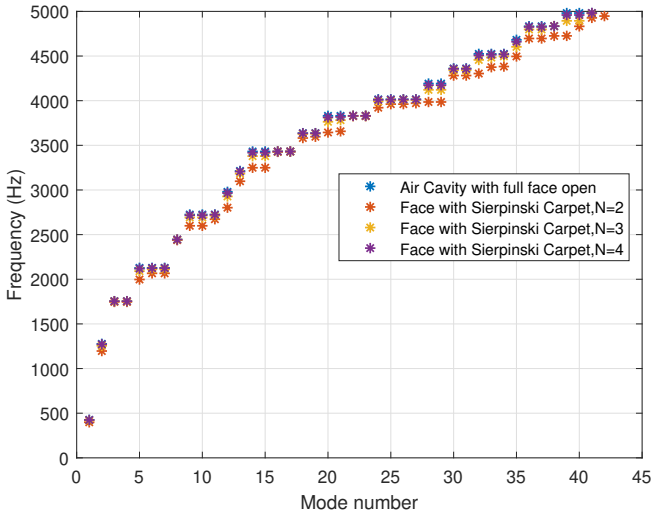

Figure 12: Eigen-frequencies for $L_z = 200$ mm

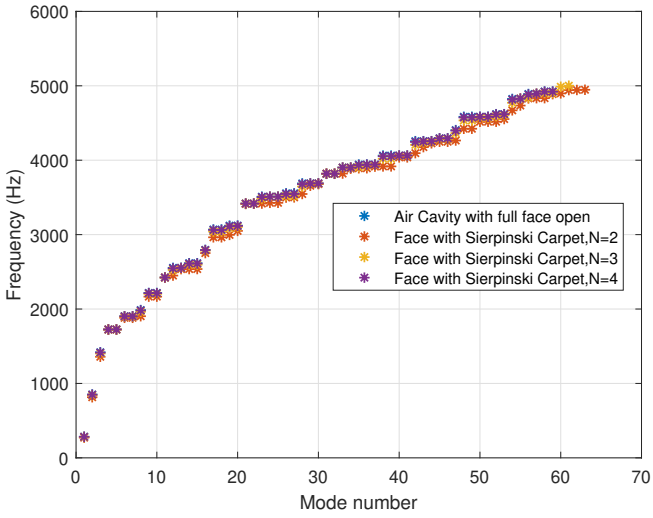

Figure 13: Eigen-frequencies for $L_z = 300$ mm

We observe that the number of modes increase on increasing the length of the cavity L_z, which is a direct consequence of Eq.(2). For a particular value of L_z, the number of modes decrease on increasing N, and the eigen-frequencies also become more similar to the case where the entire square face of the cavity is open (Eq.(2)). This is explained by the fact that as N increases, the total area of the square holes starts approaching the total area of the square face, i.e. the remaining area tends to 0 (Eq.(1)). Note that we get repeated eigen-frequencies due to the square geometry chosen, i.e. $L_x = L_y$. The next task is to make a finite element (FE) model of an impedance tube with a specimen of a certain thickness having this fractal curve, in ABAQUS. From this, the absorption curves are obtained, with the goal of validating them through actual experiments.

4 FE model of the Impedance Tube

The Impedance Tube apparatus is used to obtain normal incidence sound absorption coefficients as well as transmission coefficients. In the experimental setup to measure the absorption, there is a sound source at one

end, and two microphones present in front of the specimen. We can either directly have a rigid wall backing, or an air gap followed by a rigid wall backing, just behind the specimen. A schematic of a typical set-up is shown below.

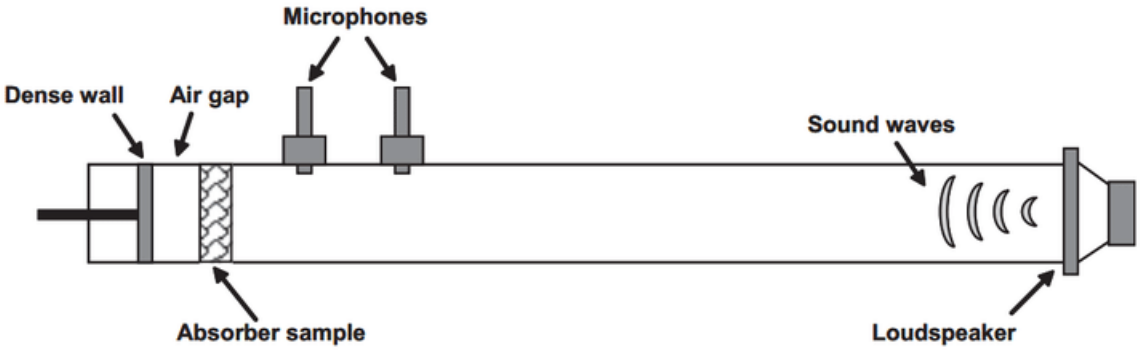

Figure 14: Impedance Tube Schematic

The two microphones are used to decompose the incident and reflected wave amplitudes, p_i and p_r respectively. The sound reflection coefficient R, and hence the sound absorption coefficient α, are then given by

$$R = \frac{p_i}{p_r}$$

$$\implies \alpha = 1 - |R|^2$$

To mimic the experiment in ABAQUS, a FE model of the impedance tube setup is designed. This consists of modelling the air inside the setup, and subsequently meshing it. We again start by sketching a square of dimensions $a \times a$, and then extruding it by a distance of d_1. Following this, the fractal curve is sketched on the square face generated after extrusion. This is then subsequently extruded by a distance d_2, which is the thickness of the specimen. We then again sketch a square face on the end of the 'holes', and extrude it by d_3. This gives the model of the impedance tube, having the specimen with an air gap followed by a rigid termination. Its schematic is shown below.

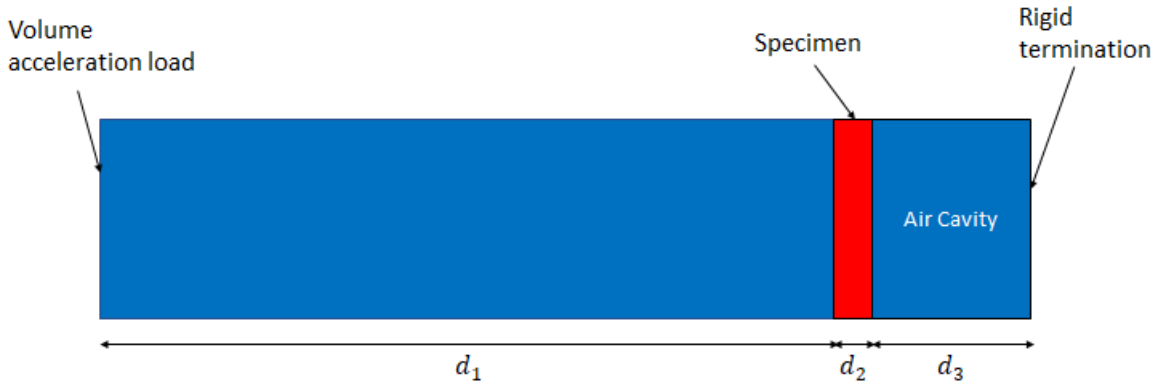

Figure 15: Schematic of impedance tube with single specimen

Coming to the material definitions, we again choose the material behaviour to be 'acoustic medium' in the 'Property' module, with density ρ and Bulk modulus B chosen to be the standard values. However, we also define volumetric drag γ, which is a flow resistance through which internal energy losses are applied. For a Sierpiński carpet of order N, we have $N + 1$ different cross sections in the model, and so we need to have $N + 1$ different material definitions. For the air in front of, and behind the specimen, the drag is defined to be

$$\gamma = 10^{-4} f^2$$

where f is the frequency in Hz. For the holes in the specimen generated after every iteration, the drag is then increased by a factor of 3. The model is finally meshed using 10-noded quadratic tetrahedral elements, with the mesh being finer in the region around the square holes. We then apply a volume acceleration load of $0.01 + 0i$ on the other square face of the tube, which mimics the speaker of the actual experiment. To mimic the pressure measurements made by the two microphones in the actual experiment, we select two nodes at distances x_1 and x_2 from the specimen, along the centreline of the tube, and record the pressure there. We now describe the procedure to calculate the absorption coefficient from this data. Let the pressures be $\tilde{P}_1$ and $\tilde{P}_2$ respectively. The auto- and cross-spectral densities of these two pressures are estimated by

$$\hat{S}_{11} = \tilde{P}_1 \tilde{P}_1^*$$

$$\hat{S}_{22} = \tilde{P}_2 \tilde{P}_2^*$$

$$\hat{S}_{12} = \hat{C}_{12} + i\hat{Q}_{12} = \tilde{P}_1 \tilde{P}_2^*$$

where $\hat{S}_{11}$ and $\hat{S}_{22}$ are estimates of the auto-spectral densities of the pressure at nodes 1 and 2, and $\hat{S}_{12}$ is an estimate of the cross-spectral density between the pressures at nodes 1 and 2; $\hat{C}_{12}$ and $\hat{Q}_{12}$ are the real and imaginary parts of $\hat{S}_{12}$. Once these quantities are estimated, we can solve the system of equations

$$\hat{S}_{11} = \hat{S}_{AA} + \hat{S}_{BB} + 2(\hat{C}_{AB} \cos 2kx_1 + \hat{Q}_{AB} \sin 2kx_1)$$

$$\hat{S}_{22} = \hat{S}_{AA} + \hat{S}_{BB} + 2(\hat{C}_{AB} \cos 2kx_2 + \hat{Q}_{AB} \sin 2kx_2)$$

$$\hat{C}_{12} = (\hat{S}_{AA} + \hat{S}_{BB}) \cos k(x_1 - x_2) + 2(\hat{C}_{AB} \cos k(x_1 + x_2) + \hat{Q}_{AB} \sin k(x_1 + x_2))$$

$$\hat{Q}_{12} = (-\hat{S}_{AA} + \hat{S}_{BB}) \sin k(x_1 - x_2)$$

for the unknowns $\hat{S}_{AA}$, $\hat{S}_{BB}$, $\hat{C}_{AB}$ and $\hat{Q}_{AB}$. Here, $\hat{S}_{AA}$ and $\hat{S}_{BB}$ are the auto-spectral densities of the incident and reflected waves, respectively, and $\hat{C}_{AB}$ and $\hat{Q}_{AB}$ are the real and imaginary components of the cross-spectral density $\hat{S}_{AB}$ between the incident and reflected waves. The power reflection coefficient P_r can then be estimated by

$$P_r = \frac{\hat{S}_{BB}}{\hat{S}_{AA}}$$

This gives the sound absorption coefficient as

$$\alpha = 1 - P_r$$

All this assumes 1D plane-wave propagation. However, there is an upper frequency up to which one can use this. The impedance tube can be approximated as a rectangular waveguide with dimensions $a \times a$. There exists a cut-on frequency f_c up to which we have 1D wave propagation. If the frequency of excitation exceeds f_c, higher modes also start propagating, and we might have wave propagation in both 2D and 3D, and hence the expressions derived above cannot be used. For the impedance tube, f_c is given by

$$f_c = \frac{c}{2a}$$

$$\implies f_c \approx 1700 \text{ Hz}$$

This analysis is done in ABAQUS by selecting the 'Procedure type' as 'Linear perturbation' and choosing the 'Steady-state dynamics, Direct' step, in the Step module, and then doing a frequency sweep from 100 Hz to 1700 Hz, in steps of 50 Hz. We thus have

$$f_{max} = 1700 \text{ Hz}$$

$$\implies \Omega_{max} = 0.04$$

i.e. the maximum element size should not exceed 40 mm. The load is applied by selecting 'Inward volume acceleration', from the 'Acoustic' category, in the Load module. The values of the various parameters associated with this analysis are

$$a = 100 \text{ mm}, \; d_1 = 790 \text{ mm}, \; d_2 = 10 \text{ mm}, \; d_3 = 100 \text{ mm}$$

$$x_1 = 150 \text{ mm}, \; x_2 = 200 \text{ mm}, \; N = 3$$

The FE model of the impedance tube, and its mesh in ABAQUS is shown below.

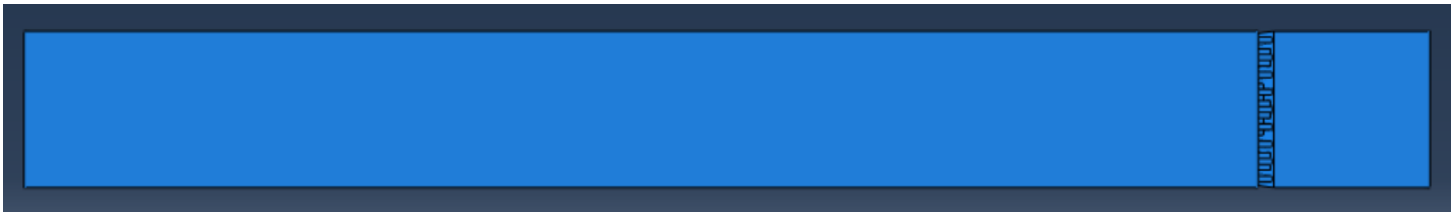

Figure 16: FE model of the impedance tube in ABAQUS

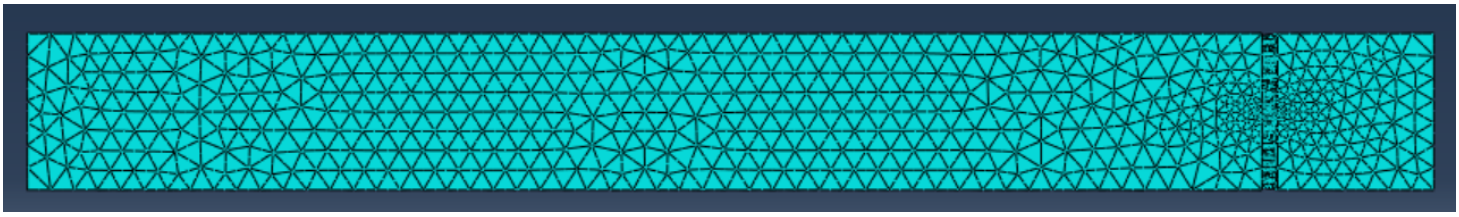

Figure 17: Mesh of the FE model

The absorption versus frequency plot for this model is now shown below.

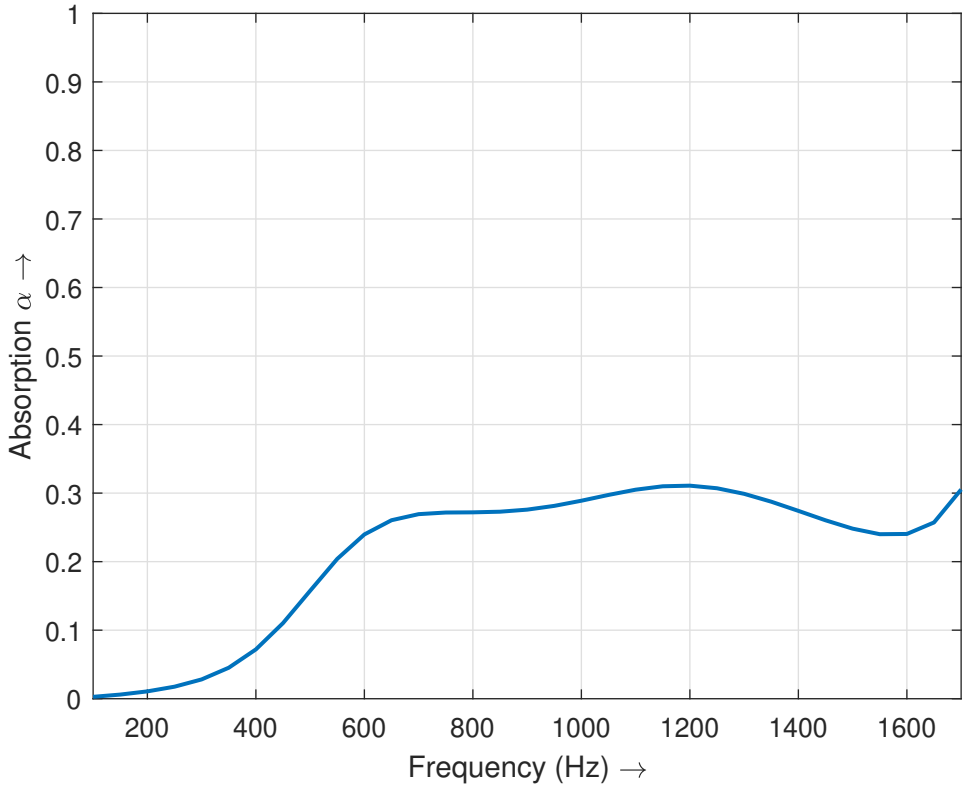

Figure 18: Absorption curve for a single specimen

From the plot, we can observe that the absorption coefficient is not very high. We look at the case where we now have two specimens instead of a single specimen in the impedance tube. The entire analysis procedure remains the same, with the only difference being that the second specimen is at a distance of d_3 from the first specimen, and the length of the air cavity is d_4. Its schematic is shown below.

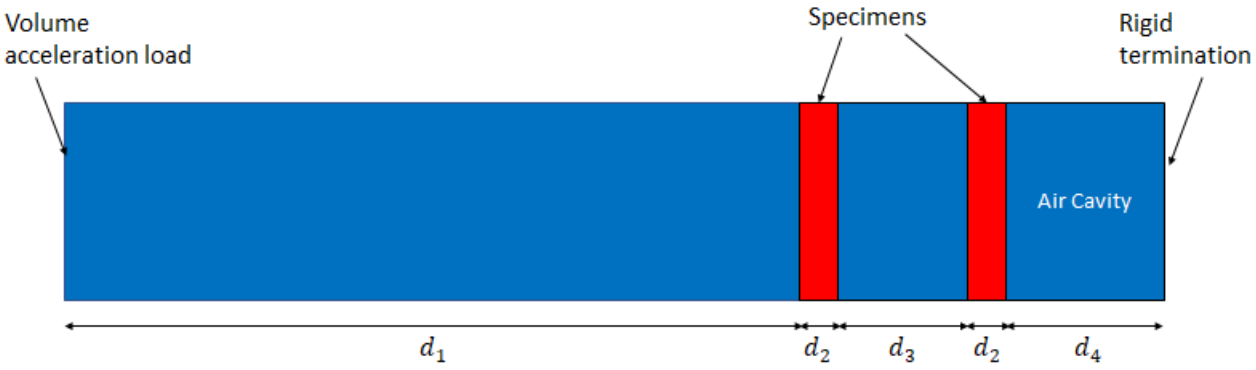

Figure 19: Schematic of impedance tube with two specimens

The values of the parameters associated with this analysis are

$$a = 100 \text{ mm}, \; d_1 = 790 \text{ mm}, \; d_2 = 10 \text{ mm}, \; d_4 = 100 \text{ mm}$$

$$x_1 = 150 \text{ mm}, \; x_2 = 200 \text{ mm}, \; N = 3$$

We investigate the effect of changing the length between the specimens, i.e. d_3, on the absorption. The values of d_3 are 50, 75 and 100 mm. The FE model for $d_3 = 75$ mm, and its mesh in ABAQUS is shown below.

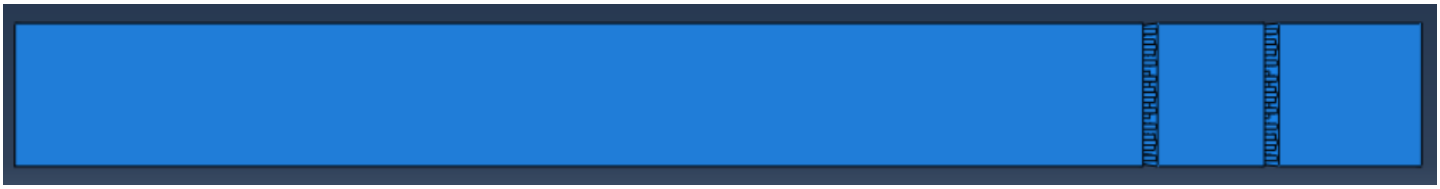

Figure 20: FE model of the impedance tube in ABAQUS

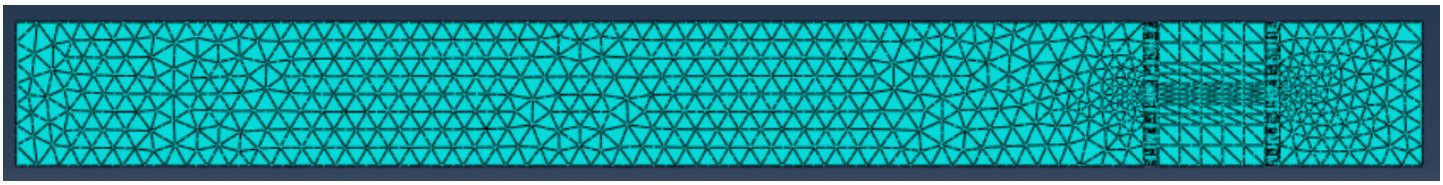

Figure 21: Mesh of the FE model

The absorption versus frequency plot for this model, for the three different values of d_3, is now shown below. This is also compared with the case when we just have a single specimen.

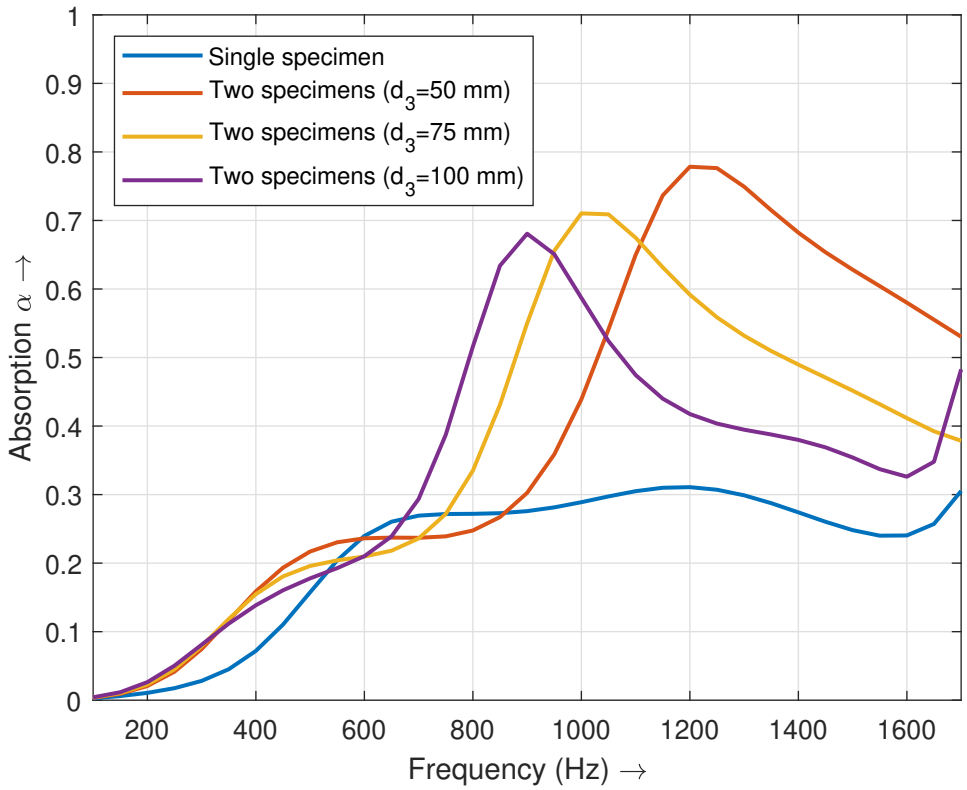

Figure 22: Absorption curves

We observe that having two specimens gives us better absorption characteristics than just a single specimen. There is also a distinct absorption peak, whose magnitude and location can be controlled by changing d_3. On decreasing d_3, the absorption peak shifts to higher frequencies and also increases in magnitude.
We now also look at the case where we have three specimens, one after the other, in the impedance tube. The additional design variable introduced is d_5, which is the distance between the third specimen and the rigid wall backing, with d_4 being the distance between the second and third specimen. The schematic is shown below.

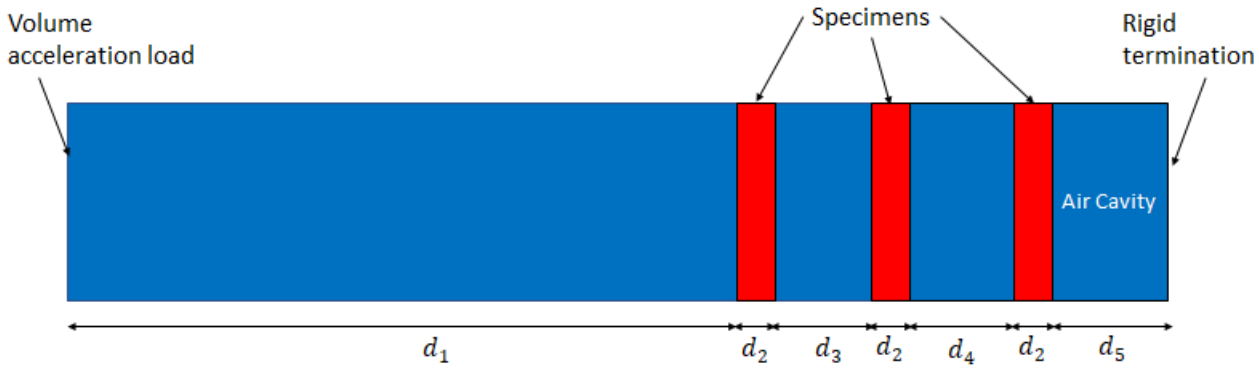

Figure 23: Schematic of impedance tube with three specimens

The values of the parameters associated with this analysis are

$$a = 100 \text{ mm}, d_1 = 790 \text{ mm}, d_2 = 10 \text{ mm}, d_3 = 100 \text{ mm}, d_4 = 100 \text{ mm}, d_5 = 100 \text{ mm}$$

$$x_1 = 150 \text{ mm}, x_2 = 200 \text{ mm}, N = 3$$

The FE model of the impedance tube with three specimens, and its mesh, is shown below.

Figure 24: FE model of the impedance tube in ABAQUS

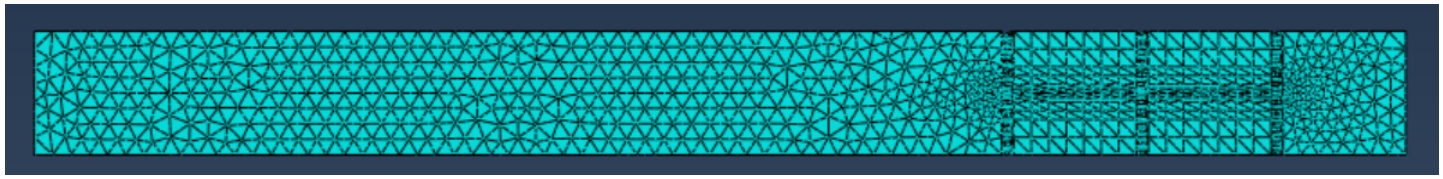

Figure 25: Mesh of the FE model

The absoprtion versus frequency plot for this model is now shown below. This is also compared with the situations investigated previously.

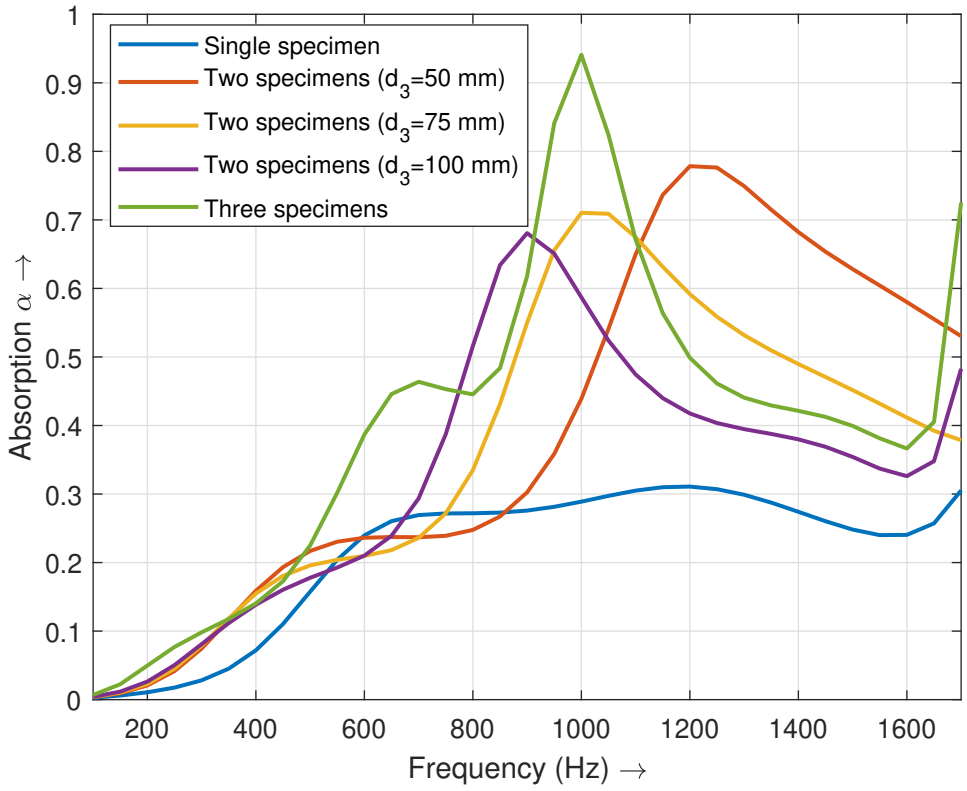

Figure 26: Absorption curves

We observe that the peak absorption value increases when we have three specimens. The performance is clearly superior in the range of 900 to 1100 Hz, though the absorption coefficient decreases after that, before increasing again at around 1600 Hz. Again, like the previous situation, the peak absorption value and its location can be tuned by changing the values of d_3, d_4 and d_5.

5 Conclusion

The use of porous fractal acoustic meta-materials for noise suppression and absorption has been investigated. The fractal curve of interest is a Sierpiński Carpet. The metamaterial is very similar in construction to a micro perforated panel (MPP) absorber, the only difference being that the perforations are replaced by the square holes of the fractal curve. All the finite-element simulations have been done in ABAQUS, with scripts written in Python to generate the complicated part geometry and set up the overall simulation. An eigen-frequency analysis of a cuboidal air cavity, which has this fractal curve on one of its faces, has been conducted. An impedance tube setup has also been mimicked, which has one or many such metamaterials one after the other, and the corresponding absoprtion curves have been obtained. It was observed that in general, the peak absorption value increases as the number of metamaterials/specimens are increased in the impedance tube. Also, for the case where we have two or more metamaterials one after the other, the location of the peak absorption value can be altered by changing the distances between the metamaterials. For example, in the case of two metamaterials, the location of the peak shifts to higher frequencies as the distance between the two metamaterials is decreased. The next task is to validate these results through actual experiments, and also to check the validity of the expression used for the volumetric drag. Since the expression used is quite arbitrary, the experiments can confirm the correctness of the same. If there is not much difference between the two results, the expression can be used for further studies. But if there is considerable difference, some different expressions need to be considered (either by changing the functional form, or by changing the proportionality constant) , until the two results somewhat match. The absoprtion curves can then be updated, and can be finally compared with different sound absorbers already in use.

6 References

1) Xianfeng Man, Baizhan Xia, Zhen Luo, Jian Liu, Kun Li and Yonghong Nie, Engineering three-dimensional labyrinthine fractal acoustic metamaterials with low-frequency multi-band sound suppression, The Journal of the Acoustical Society of America, 2021.
2) Xinzhe Zhao, Guoqiang Liu, Chao Zhang, Dong Xia and Zhumao Lu, Fractal acoustic metamaterials for transformer noise reduction, Applied Physics Letters, 2018.
3) Baizhan Xia, Liping Li, Jian Liu and Dejie Yu, Acoustic Metamaterial With Fractal Coiling Up Space for Sound Blocking in a Deep Subwavelength Scale, Journal of Vibration and Acoustics, 2018.
4) J.F. Ning, S.W. Ren and G.P. Zhao, Acoustic properties of micro-perforated panel absorber having arbitrary cross-sectional perforations, Applied Acoustics, 2016.
5) A.F. Seybert and D.F. Ross, Experimental determination of acoustic properties using a two-microphone random excitation technique, The Journal of the Acoustical Society of America, 1977.
6) Source for Figure 14: `https://www.researchgate.net/figure/Sound-absorption-experiment-setup-using-an-impedance-tube-and-the-twomicrophone_fig40_318858709`

X————X————X